Acoustic Wind-Tunnel Measurements with a Highly Directional Microphone

F. -R. Grosche,* H. Stiewitt,† and B. Binder‡
Deutsche Forschungs-und Versuchsanstalt für Luft- und Raumfahrt, Aerodynamische Versuchsanstalt Göttingen, Göttingen, West Germany

The potential of the acoustic mirror as a highly directional microphone system for sound source location and discrimination from background noise in aeroacoustic wind-tunnel tests was investigated through measurements of the noise of a model source in the open test section of a low-speed wind tunnel, the mirror being positioned outside the flow. The acoustic performance of the mirror is affected by scattering and refraction of the sound waves in the free shear layer of the tunnel, but these effects were found to be important only at high sound frequencies where they approximately compensate the increase of both the spatial resolution and gain factor of the mirror with frequency.

Nomenclature

A = 3.7 m, distance from sound source to mirror, see Fig. 5
a_0 = 345 m/sec, ambient sound velocity
b = distance between center and first minimum of diffraction pattern, mm, see Figs. 4 and 5
D = 1m, diameter of the mirror, see Fig. 5
f = frequency, center-frequency of 1/3 octave bands, kHz
G = $L_M - L_{R0}$, effective gain factor, dB, see Fig. 4
G_0 = $L_{M0} - L_{R0}$, effective gain factor at zero wind velocity, dB, see Fig. 4
I = sound intensity (in 1/3 octave bands), W/m^2
I_M = sound intensity in the maximum of the diffraction pattern, W/m^2
L = sound-pressure level, dB, re $2\cdot10^{-5}$ N/m^2 (in 1/3 octave bands)
L_M = sound-pressure level in the maximum of the diffraction pattern, dB, see Fig. 4
L_{M0} = sound pressure level in the maximum of the diffraction pattern at zero wind velocity, dB
L_R = sound-pressure level measured by the omnidirectional reference microphone, dB, see Figs. 1 and 3
L_{R0} = sound-pressure level measured by the omnidirectional reference microphone at zero wind velocity, dB
M = U_∞/a_0, Mach number of the wind tunnel flow
R = radius of curvature of the mirror, 1m
U_∞ = wind velocity in the test section of the tunnel, m/sec
w = half-width of the diffraction pattern, mm, see Figs. 4 and 11
w_0 = half-width of the diffraction pattern at zero wind velocity, mm, see Figs. 4 and 6
x,y,z = Cartesian coordinates, m, see Fig. 1
$x_{\min}$ = b, mirror position at the first minimum of the diffraction pattern, m, see Fig. 5
y_T = 1.5 m, distance between sound source and boundary of the wind-tunnel flow, see Fig. 8
$\alpha_{\min}$ = angle of the first minimum of the diffraction pattern, deg, see Fig. 5
δ = width of the free shear layer of the tunnel flow at the x position of the sound source, $\approx$0.48 m
ΔL = $L_{M0} - L_M$, difference in sound levels, dB, see Fig. 4
λ = a_0/f, acoustic wavelength

Presented as Paper 76-535 at the 3rd AIAA Aero-Acoustics Conference, Palo Alto, Calif., July 20-23, 1976; submitted Feb. 1, 1977; revision received Aug. 2, 1977.
Index category: Aeroacoustics.
*Scientist. Member AIAA.
†Scientist.
‡Research Engineer.

I. Introduction

THE relative mainstream flow past aircraft or ground vehicles in motion produces aerodynamic noise, e.g., through the pressure fluctuations occurring in turbulent boundary layers and flow separation regimes.[1-4] Also, the sound radiation of sources like fans, propellers, and jet exhausts can be altered significantly by the external flowfield due to the forward speed of the vehicle.[5-13]

Wind-tunnel tests appear to be a convenient method of investigating these effects under controlled and repeatable conditions.[11-17] Unfortunately, the background noise level of most existing wind tunnels, which were designed for aerodynamic measurements only, is rather high. Therefore, these tunnels need acoustic treatment to reduce reverberation and to prevent the noise of the fan and tunnel circuit to reach the test section.

Another attractive possibility to improve the signal-to-noise ratio in such wind tunnels is to use directional microphones that enhance the sound signal received from the model. In addition, highly directional microphone systems would allow us to locate individual sound sources or to determine the source distributions of aeroacoustic models.

The present paper describes investigations conducted to establish the feasibility of applying such a directional

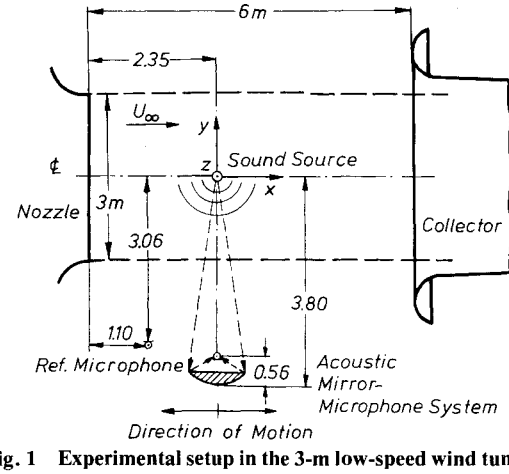

Fig. 1 Experimental setup in the 3-m low-speed wind tunnel.

microphone system to aeroacoustic tests in an open jet wind tunnel.

The method investigated is the acoustic mirror technique, which already has been used successfully to determine the distribution of sound source intensities in turbulent jets under static conditions.[18,19] The sound waves emanating from a volume element of the source distribution are focused upon a microphone by means of a large concave mirror, both mirror and microphone being located in the acoustic far field. The spatial resolution and the gain factor of the system are limited mainly by diffraction of the sound waves at the edge of the mirror, if there is no significant flow between sound source and mirror system. More details of the acoustic mirror technique are given in Ref. 18. In the case we are considering here, the acoustic mirror system is positioned outside of the open test section of a low-speed wind tunnel, receiving sound from a source (or sources) within the tunnel flow (see Fig. 1). In this case, the sound waves propagating to the mirror are refracted and scattered by the free shear layer of the wind tunnel.

The main objective of the tests described in this paper was to study the influence of these effects of the flow upon the acoustic performance of the mirror system.

II. Measurements

The test setup and the coordinate system are shown in Fig. 1. The distributions of sound intensities in the image of a point source of sound on the wind-tunnel centerline were measured at different wind velocities $0 \leq U_\infty \leq 60$ m/sec by moving the mirror-microphone system parallel to the wind-tunnel axis and recording the 1/3 octave-sound pressure levels L as function of the mirror position x. At the same time, the 1/3 octave spectrum of the sound pressure level L_R in the vicinity of the mirror-microphone system was measured by an omnidirectional "reference microphone" (see Fig. 1) to determine the gain factor of the mirror and the ambient noise level produced by the wind tunnel itself.

After these measurements, some experiments were carried out to investigate sources of airframe noise. The point source of sound was replaced by a sting-supported model of a fighter aircraft with movable flaps that was available for these preliminary tests from earlier aerodynamic measurements. The model was turned by 90 deg about its longitudinal axis so that its lower side faced the mirror. The wing span of the model was 1.5 m. The flaps could be set to angles of 0 and 30 deg. A schematic view of the model is presented in the upper parts of Figs. 15 and 16. Also indicated here is the traverse of the focus of the mirror over wing and tailplane.

III. Apparatus

The tests were conducted in the 3-m low-speed wind tunnel of DFVLR-AVA Göttingen. The tunnel has a closed return circuit with an open test section 6 m long and a quadratic nozzle exit area of 3×3 m^2, as indicated in Fig. 1.

Vortex generators are fitted to the edge of the nozzle to prevent low-frequency pulsations of the flow. The wind tunnel is built of concrete and steel; no sound absorbing linings were installed during the tests. Therefore, the reverberation time was approximately 1-5 sec for the frequency range of interest. The maximum wind velocity of the tunnel is $U_\infty = 65$ m/sec; the turbulence level is about 0.2%. A more detailed description of the wind tunnel can be found in Refs. 19 and 20.

A very small treble loudspeaker, the diaphragm having a diameter of about 25 mm, was positioned on the centerline of the wind tunnel 2.35 m from the nozzle to simulate a point source of sound (see Fig. 1). The loudspeaker was mounted on a vertical beam. Streamlined fairings were attached to the loudspeaker and supporting beam to suppress vibrations and spurious noise radiation due to unsteady flow separations. The loudspeaker was connected via a high-pass filter and a power amplifier to a noise generator producing white noise in the frequency range 0.1-100 kHz (see the block diagram in Fig. 2). The rms-voltage at the loudspeaker was measured and kept constant during the tests.

The acoustic mirror-microphone system is shown in the lower part of Fig. 1. A spherical mirror made of fiberglass was mounted on a traversing unit, which allowed the system to be moved with constant velocity in the directions parallel and normal to the centerline of the wind tunnel, The diameter of the mirror was $D = 1$ m, its radius of curvature was also $R \cong 1$ m. A 1/4-in. B&K condenser microphone pointing to the center of the mirror was positioned on the mirror axis by means of a strutted arm attached to the supporting frame of the mirror. The mirror axis was normal to the centerline of the wind tunnel for all measurements, as indicated by Fig. 1.

Figure 2 presents the instrumentation: The signal of the mirror microphone was amplified, filtered by means of a 1/3 octave filter, and recorded by a graphic level recorder. The level recorder was started simultaneously with the motor of the traversing unit, and event marks were put on the record automatically when the mirror passed through equidistant

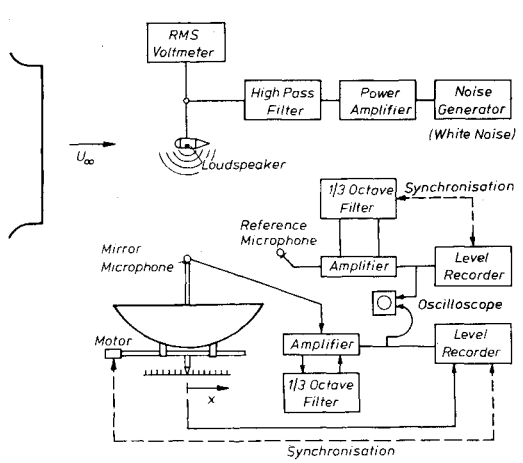

Fig. 2 Block diagram of the instrumentation.

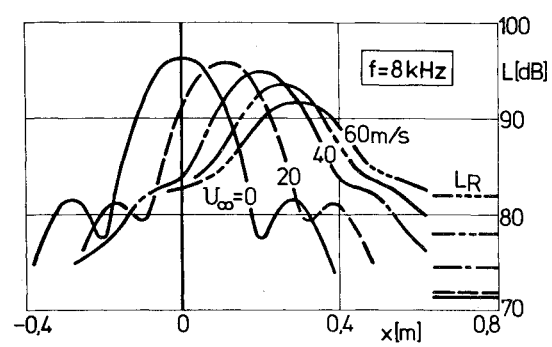

Fig. 3 Diffraction patterns of the sound source in the wind tunnel measured in the 1/3 octave band with center frequency $f = 8$ kHz at different wind velocities U_∞.

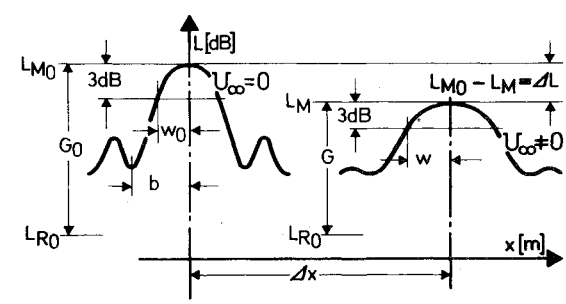

Fig. 4 Characteristics of the diffraction patterns evaluated from the measured data.

positions. The records thus display the measured sound pressure level L in the selected frequency band as function of the mirror position x.

A 1/4-in. B&K microphone was used as the omnidirectional "reference microphone" shown in Fig. 1 for measuring the ambient sound pressure level in the vicinity of the mirror microphone. The signal was analyzed by a conventional B&K 1/3 octave filter-level recorder combination (see Fig. 2).

IV. Results

A typical set of measured data is presented in Fig. 3, which shows the diffraction patterns of the sound source on the tunnel axis measured at different wind velocities U_∞ in the 1/3 octave band with center frequency $f = 8$ kHz. The curves for $U_\infty = 10$ m/sec and $U_\infty = 30$ m/sec were also measured but are omitted for the sake of clarity of the diagram. The reference sound-pressure levels L_R ($f = 8$ kHz) determined by the omnidirectional reference microphone (see Fig. 1) are indicated on the right-hand side of the figure. Similar sets of measurements were made for other 1/3-octave bands with center frequencies $f = 2, 4, 5, 10, 16, 25$, and 31.5 kHz.

The following characteristics of the diffraction patterns were evaluated from these test results (see Fig. 4):

a) For wind velocity $U_\infty = 0$:

1) Width of the diffraction pattern as function of frequency f, defined by the distance b between the maximum and the first minimum of the diffraction pattern and by the half-width w_0 between the center of the pattern and the point where the sound intensity has decreased by 3 dB or 50%.

2) Effective gain factor $G_0 = L_{M0} - L_{R0}$ of the mirror as function of frequency, with L_{M0} being the sound-pressure level measured by the mirror-microphone in the maximum of the diffraction pattern and L_{R0} being the level measured by the reference microphone at $U_\infty = 0$.

b) For wind velocities $U_\infty \neq 0$:

1) Apparent shift Δx of the source position with wind velocity U_∞.

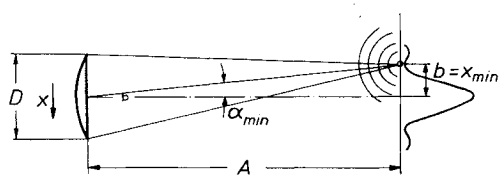

$\sin\alpha_{min} = 1.22\frac{\lambda}{D}$ (Diffraction at a Circular Aperture)

Fig. 5 Diffraction of sound waves at the edge of the mirror.

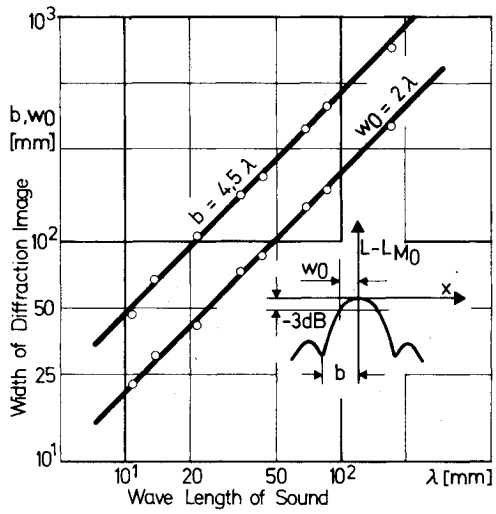

Fig. 6 Width of the diffraction pattern of the sound source as a function of the acoustic wavelength for zero wind velocity $U_\infty = 0$.

2) Half-width w of the diffraction pattern.

3) Reduction $\Delta L_M = L_{M0} - L_M$ of the sound-pressure level in the center of the diffraction pattern as compared to the level L_{M0} for $U_\infty = 0$, and effective gain factor $G = L_M - L_{R0}$.

A. Spatial Resolution and Effective Gain Factor of Mirror-Microphone System at Zero Wind Velocity

The distance b between the first minimum of the diffraction pattern and the center of the pattern can be estimated readily from the well-known equation for the angle α_{min} of the first minimum in the case of a circular aperture, see, e.g., Ref. 21:

$$\sin\alpha_{min} = 1.22\frac{\lambda}{D} \tag{1}$$

According to Fig. 5, the sound-pressure level at the mirror-microphone becomes a minimum when the mirror is shifted relative to the position of the sound source by

$$x_{min} \triangleq b = A \cdot \tan\alpha_{min} \approx A \cdot \sin\alpha_{min} = 1.22\, A\frac{\lambda}{D} \tag{2}$$

With a distance A between mirror and sound source of $A \approx 3.7$ m, and a mirror diameter of $D = 1.0$ m, one obtains

$$b = 4.5\lambda \tag{3}$$

This is verified quite accurately by the experimental results plotted in Fig. 6, which also shows the measured half-width w_0 as a function of the acoustic wavelength. According to Fig. 6, and again in accordance with theoretical estimates, w_0 is related to b and λ by

$$w_0 = 0.45\ b = 2.02\lambda \tag{4}$$

The effective gain factor $G_0 = L_M - L_{R0}$ of the mirror is presented in Fig. 7 as function of sound frequency f. The gain factor increases with 6 dB/octave. This was expected since the area of the diffraction pattern varies with $b^2 \sim \lambda^2$ and thus the sound intensity in the pattern should increase with $1/\lambda^2 \sim f^2$ if the sound power output of the source is kept constant. The term "effective" gain factor is introduced because the reference level L_{R0} was not measured in the acoustic free field but in a partly reverberant field. Under free-field conditions the reference level L_{R0} would be lower and therefore the true gain factor should be higher than the effective gain factor.

B. Effects of Wind Tunnel Flow on Measurements with Mirror-Microphone System

Apparent Shift of Source Position

The maximum of the diffraction pattern moves in the downstream direction with increasing wind velocity (see Fig.

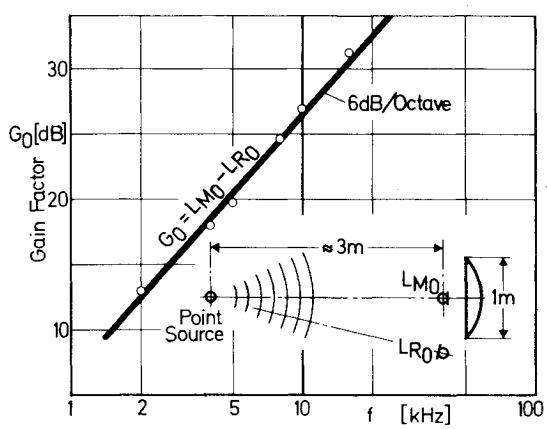

Fig. 7 Effective gain factor of the mirror as a function of sound frequency for zero wind velocity $U_\infty = 0$.

3). This is obviously due to the convection of the sound waves by the flow and to the refraction in the free shear layer of the test section.

A sound wave emitted from the source on the centerline of the tunnel is convected downstream the distance

$$\Delta x = y_T \cdot \frac{U_\infty}{a_0} \tag{5}$$

before the part radiated at 90 deg to the tunnel axis arrives at the boundary of the flow, $y_T \approx 1.5$ m (see Fig. 1). From here on, this part of the wave propagates in its original direction of about 90 deg to the tunnel axis, and is focused upon the microphone by the concave mirror when the mirror arrives at the position $x = \Delta x$.

The measured displacement Δx of the maxima of the diffraction patterns normalized by the half-width of the wind-tunnel nozzle, $y_T = 1.5$ m, is plotted over the flow Mach number $M = U_\infty / a_0$ in Fig. 8. The measured data can be represented by

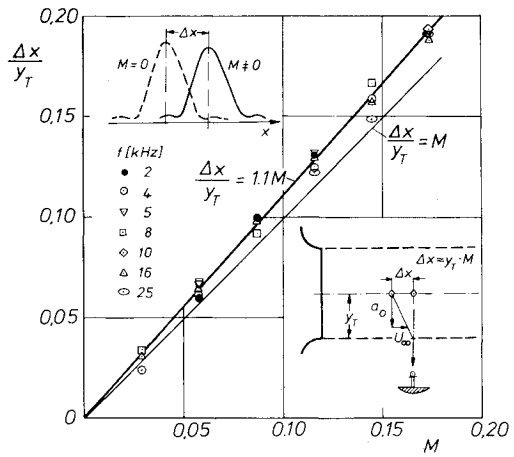

Fig. 8 Apparent shift of the position of the sound source as a function of flow Mach number $M = U_\infty / a_0$.

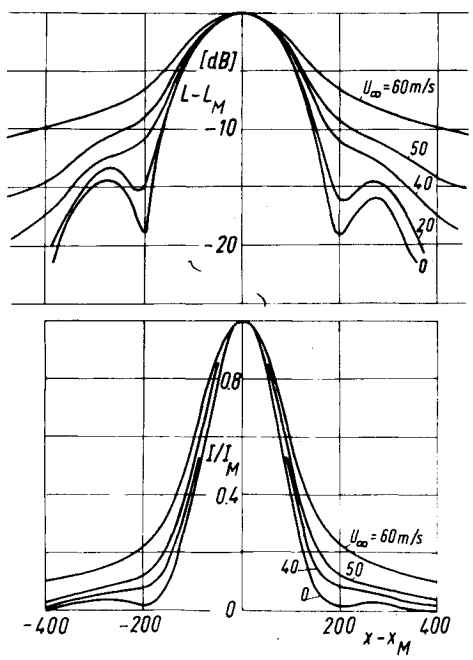

Fig. 9 Variation of the shape of the diffraction pattern with wind velocity. Center frequency of the 1/3 octave band: $f = 8$ kHz. Upper part: sound pressure levels. Lower part: intensities. $10 \log I/I_M = L - L_M$.

$$\frac{\Delta x}{y_T} = 1.1 \frac{U_\infty}{a_0} \tag{6}$$

which comes quite close to the estimate Eq. (5). The result appears to be almost independent of sound frequency within the frequency range 2 kHz $\leqq f \leqq$ 25 kHz. A more detailed analysis will be made on the basis of existing theories, e.g., Ref. 22.

Broadening of Diffraction Pattern

The variation of the shape of the diffraction pattern with wind velocity U_∞ is demonstrated by Fig. 9, which shows the normalized sound-pressure levels $L(x) - L_M$ and corresponding sound-intensity profiles $I(x)/I_M$ measured in the 8 kHz-1/3 octave band (see also Fig. 3). Apparently the sound is scattered by the turbulent shear layer. At low wind velocities, the minima of the pattern are smoothed out, but the upper part of the distributions remains almost unchanged. This is no longer true for wind velocities $U_\infty \geqq 40$ m/sec, but still mainly the lower part of the patterns is affected. The increase of the normalized half-width w/λ of the diffraction pattern with the Mach number $M = U_\infty / a_0$ of the wind tunnel is given by Fig. 10 for different sound frequencies. The broadening of the intensity profiles becomes more pronounced for higher sound frequencies f. This is due to the

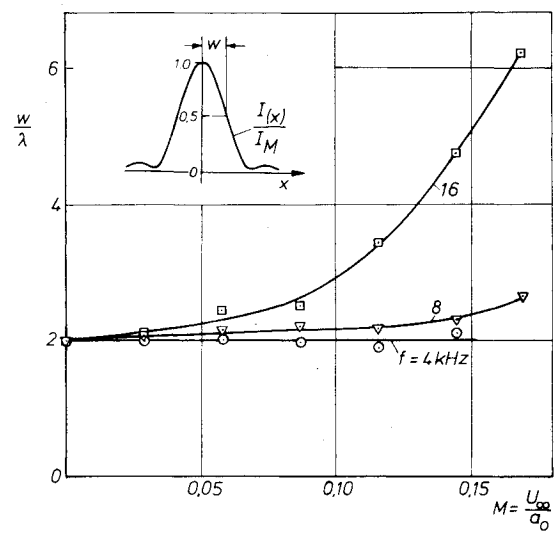

Fig. 10 Normalized half-width w/λ of the diffraction pattern as a function of flow Mach number at different sound frequencies.

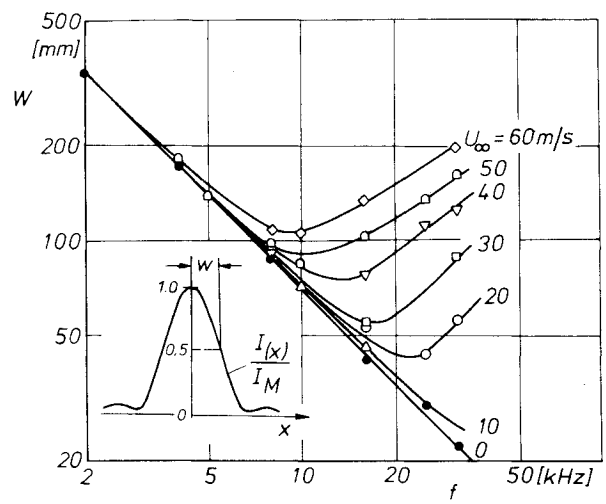

Fig. 11 Half-width of the diffraction pattern of a sound source in the wind tunnel as a function of sound frequency at different wind velocities U_∞.

greater ratio of turbulence scale in the shear layer to the acoustic wavelength $\lambda = a_0/f$, which leads to a stronger scattering of sound by the turbulent region; compare with Ref. 23. A quite reasonable correlation of the experimental results could be obtained by plotting w/λ vs $M \cdot \delta/\lambda$, where δ is the width of the free shear layer, but this cannot be discussed in detail in the present paper.

The effect of the wind velocity on the spatial resolution of the mirror-system is summarized in Fig. 11, which shows the half-width w as a function of sound frequency for different flow velocities. The straight line, for $U_\infty = 0$, corresponds to the lower line $w_0 = 2.02\lambda$ of Fig. 6. For a given wind velocity, the half-width of the diffraction pattern at first decreases with increasing frequency, following the curve for $U_\infty = 0$, until it reaches a minimum, the position of which depends on the wind velocity. From this point on, w increases again $\sim f^{0.6}$ for $U_\infty = 60$ m/sec and approximately $\sim f$ for $U_\infty \leqq 40$ m/sec.

At the highest wind velocity and frequency investigated ($U_\infty = 60$ m/sec, $f = 31.5$ kHz) the half-width of the diffraction pattern of the point source of sound was $w \approx 0.2$ m, which is about the same as the half-width at 4 kHz for zero wind velocity (see Fig. 11). Thus, the dependence of w_0 on sound frequency is counterbalanced to a certain extent by the effect of wind velocity. The loss in spatial resolution of the mirror system at the higher sound frequencies is therefore not considered a serious hindrance for the application of the system to aeroacoustic wind-tunnel tests.

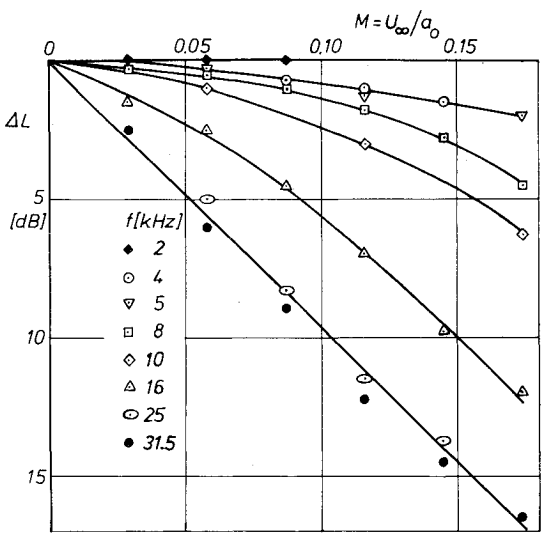

Fig. 12 Decrease $\Delta L = L_{M0} - L_M$ of the sound-pressure level L_M in the maximum of the diffraction pattern with increasing flow Mach number.

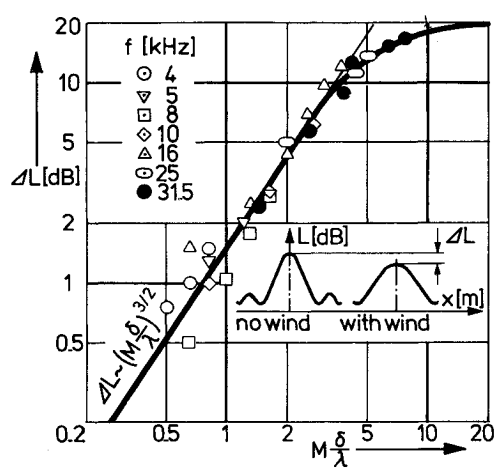

Fig. 13 Decrease $\Delta L = L_{M0} - L_M$ of the sound-pressure level L_M in the maximum of the diffraction pattern as a function of $(M \cdot \delta/\lambda)$ with δ = width of the free shear layer of the wind tunnel.

Reduction of the Effective Gain Factor

The maxima L_M of the diffraction patterns of the sound source in the wind tunnel fall off with increasing wind velocity U_∞ (see Figs. 3 and 4). This is considered to be due mainly to the scattering of the sound waves by the turbulent free shear layer of the wind tunnel.

The loss $\Delta L = L_{M0} - L_M$, where L_{M0} is the maximum level at zero wind velocity, is presented in Fig. 12 as a function of $M = U_\infty/a_0$ for different sound frequencies. Again, as with the broadening of the diffraction pattern, the influence of U_∞ increases markedly with sound frequency, and again a reasonable correlation of the data was obtained by plotting ΔL as a function of $M \cdot \delta/\lambda$ (see Fig. 13). According to this graph, the reduction of sound-pressure level in the maximum of the diffraction pattern is

$$\Delta L \sim \left(M \cdot \frac{\delta}{\lambda}\right)^{1.5} \tag{7}$$

over a wide range of M and λ or U_∞ and f, respectively.

In analogy to Fig. 11, regarding the half-width of the diffraction pattern, Fig. 14 shows the effective gain factor $G = L_M - L_{R0}$ of the mirror system at different wind velocities as a function of the sound frequency. With flow, the gain factor deviates at higher frequencies from the 6 dB/octave straight line for $U_\infty = 0$ and becomes approximately constant. For $U_\infty = 60$ m/sec, the gain factor remains about 20 dB for all frequencies above $f = 6$ kHz. For $U_\infty = 30$ m/sec, the maximum gain factor is close to 27 dB and is reached at $f \geq 12$ kHz (see Fig. 14). Thus the reduction of the gain by the scattering of sound in the free shear layer of the wind tunnel appears to be just sufficient to compensate, at higher frequencies, for the 6 dB/octave increase inherent in the mirror system.

Therefore, the gain factor remains high enough over the entire frequency range, even at the maximum wind velocity $U_\infty = 60$ m/sec, to enhance the signal of the model sound source by more than 18 dB (for $f > 4$ kHz). This means that even a model source producing a sound pressure level about 15 dB lower at the microphone position than the background noise level of the tunnel could be detected by the mirror-microphone system without difficulty.

C. Some Results of Experiments to Investigate Sources of Airframe Noise

The sting-supported aircraft model used in the tests is sketched in the upper parts of Figs. 15 and 16. In the lower

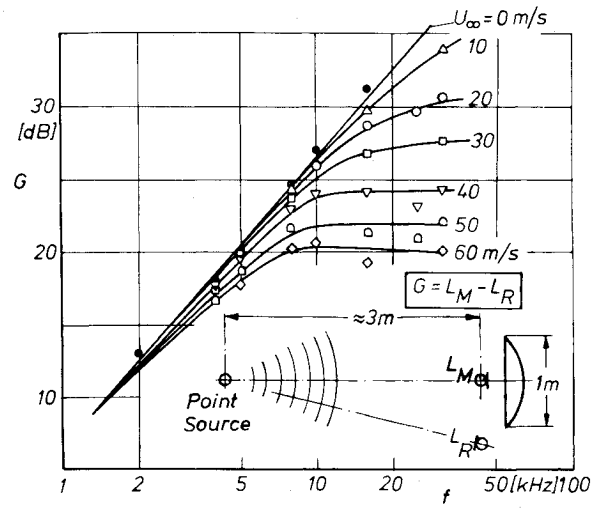

Fig. 14 Effective gain of the mirror as a function of sound frequency at different wind velocities U_∞.

part of the graphs, the sound intensity measured by the mirror-microphone in a 1/3 octave band is plotted as function of the position of the focus of the mirror. The focus position was corrected for the convection effect discussed in Sec. IV. B according to Eq. (6):

$$x' = x - \Delta x = x - 1.1 y_T M \tag{8}$$

with $y_T = 1.5$ m. No corrections for spatial resolution and gain factor were applied so far to the sound intensities measured by the mirror-microphone. Therefore, these preliminary plots indicate only the position and relative strength of the sound sources along the traverse of the mirror focus illustrated in the figures. The wind velocity was $U_\infty = 45$ m/sec for all measurements. The results presented in Fig. 15 for the 1/3 octave band with center frequency $f = 16$ kHz were obtained with the model at zero angle of attack, $\alpha = 0$ deg. The lower curve pertains to the configuration "landing flaps up," $\alpha_{Flap} = 0$ deg. In this case, the measured sound pressure level is essentially independent of the axial position of the mirror within the range investigated. This indicates that the ambient noise of the tunnel masks the sound radiation of the clean model at zero angle of attack in the selected frequency band. The upper curve gives the results with flaps set to $\alpha_{Flap} = 30$ deg. This curve clearly shows a marked peak of sound radiation at the position of the flap, followed by a second peak of radiation at the leading edge of the tailplane. This second source is due to the fact that, with the given combination of $\alpha = 0$ deg and $\alpha_{Flap} = 30$ deg, the turbulent downwash of the flap hits the low-mounted tailplane.

The source distributions measured at $\alpha = 28$ deg and $\alpha_{Flap} = 0$ deg or $\alpha_{Flap} = 30$ deg are given in Fig. 16. With flaps up, a strong noise radiation is found at the leading edge of the wing, probably caused by a separation bubble at the leading edge. A much weaker source at the trailing edge of the wing is indicated by a small hump of the curve. With flaps down, $\alpha_{Flap} = 30$ deg, sound is generated very strongly again at the flaps, as shown by the upper curve of Fig. 16. Also, the sound radiation at the leading edge of the wing is significantly amplified. This can be explained by the higher local flow velocity due to the increased circulation with flap setting $\alpha_{Flap} = 30$ deg.

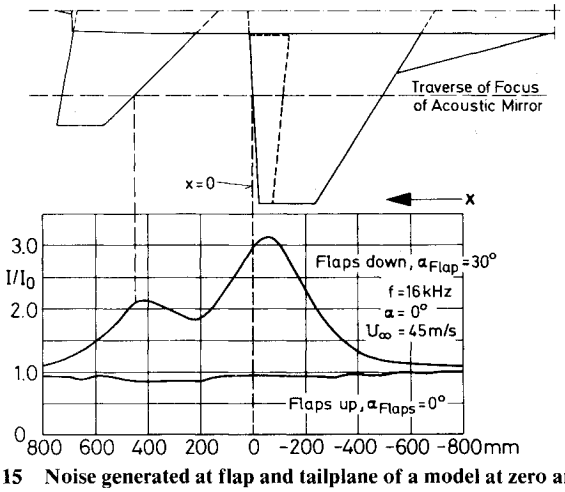

Fig. 15 Noise generated at flap and tailplane of a model at zero angle of attack and different flap settings.

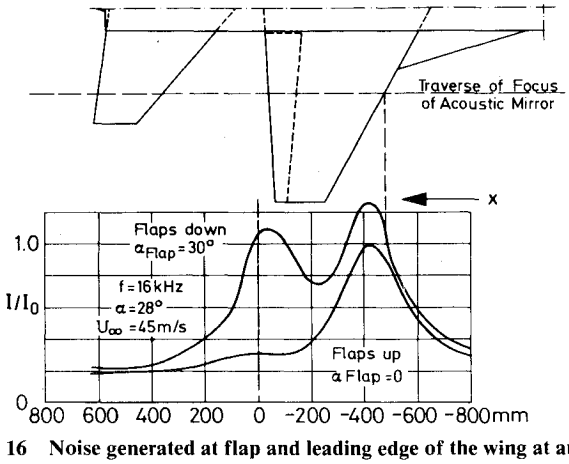

Fig. 16 Noise generated at flap and leading edge of the wing at angle of attack $\alpha = 28$ deg and different flap settings.

These examples illustrate the possibilities to localize and identify sound sources on complex aeroacoustic wind-tunnel models and to determine their relative intensity. More work is in progress to calculate also the absolute intensity distributions of the sound sources by correcting the measured data for the limited spatial resolution and gain of the mirror system.

V. Conclusions

The applicability of the acoustic mirror technique to sound source location and discrimination from background noise in aeroacoustic wind-tunnel tests was investigated through measurements of the sound emitted by a model source in the open test section of a low-speed wind tunnel.

The acoustic performance of the mirror-system is affected by the tunnel flow. The apparent center of radiation is shifted downstream by a well-defined distance proportional to the wind velocity and to the distance of the sound source from the boundary of the flow. This effect is essentially independent of sound frequency. The spatial resolution and the gain factor of the mirror are diminished mainly by the scattering of sound in the turbulent free shear layer of the tunnel flow. The losses grow with wind velocity and frequency of sound. They are significant only at higher frequencies, where they approximately compensate the steep increase of both resolution and gain factor characteristic of the mirror system at zero wind velocity. Therefore, resolution and gain factor remain sufficiently high within the frequency range of interest.

Because of these results and since the apparent shift of source position with wind velocity can be readily corrected for, the acoustic mirror technique is considered suitable for measurements in low-speed wind tunnels with open test section.

Acknowledgment

This research was in part sponsored by the Deutsche Forschungsgemeinschaft (DFG).

References

[1] Fethney, P., "An Experimental Study of Airframe Self-Noise," AIAA Paper 75-511, 1975; also AIAA *Progress in Astronautics and Aeronautics—Aeroacoustics: STOL Noise; Airframe and Airfoil Noise*, Vol. 45, edited by I. R. Schwartz, 1976, pp. 379-404.

[2] Revell, J. D., "Induced Drag Effect on Airframe Noise," AIAA Paper 75-487, 1975; also AIAA *Progress in Astronautics and Aeronautics—Aeroacoustics: STOL Noise; Airframe and Airfoil Noise*, Vol. 45, edited by I. R. Schwartz, 1976, pp. 221-236.

[3] Hayden, R. E. Kadman, Y., Africk, S., and Bliss, D. B., "Diagnostic Calculations of Airframe Noise," AIAA Paper 75-485, 1975; also AIAA *Progess in Astronautics and Aeronautics—Aeroacoustics: STOL Noise; Airframe and Airfoil Noise*, Vol. 45, edited by I. R. Schwartz, 1976, pp. 179-202.

[4] Heller, H. H. and Bliss, D. B., "The Physical Mechanism of Flow Induced Pressure Fluctuations in Cavities and Concepts for their Suppression," AIAA Paper 75-491, 1975; also *AIAA Progress in Astronautics and Aeronautics—Aeroacoustics: STOL Noise; Airframe and Airfoil Noise*, Vol. 45, edited by I. R. Schwartz, 1976, pp. 281-296.

[5] Gerend, R. P. and Schairer, G. S., "Designing for Noise Reduction," RAS Symposium on The Impact of Economics on the Design and Operation of Quieter Aircraft, April 1975, London.

[6] Lowrie, B. W., "Simulation of Flight Effects on Aero Engine Fan Noise," AIAA Paper 75-463, 1975; also AIAA *Progress in Astronautics and Aeronautics—Aeroacoustics: Fan Noise and*

Control; Duct Acoustics; Rotor Noise, Vol. 44, edited by I. R. Schwartz, New York, 1976, pp. 139-158.

[7]Merriman, J. E. and Good, R. C., "The Effect of Forward Motion on the Acoustic Characteristics of Fan Noise," AIAA Paper 75-464, 1975; also AIAA *Progress in Astronautics and Aeronautics —Aeroacoustics: Fan Noise and Control; Duct Acoustics; Rotor Noise*, Vol. 44, edited by I. R. Schwartz, New York, 1976, pp. 159-180.

[8]Roundhill, J. P. and Schaut, L. A., "Model and Full Scale Test Results Relating to Fan Noise In-Flight Effects," AIAA Paper 75-465, 1975; also AIAA *Progress in Astronautics and Aeronautics —Aeroacoustics: Fan Noise and Control; Duct Acoustics; Rotor Noise*, Vol. 44, edited by I. R. Schwartz, New York, 1976, pp. 181-208.

[9]Bushell, K. W., "Measurement and Prediction of Jet Noise in Flight," AIAA Paper 75-461, 1975; also AIAA *Progress in Aeronautics and Aeronautics—Aeroacoustics: Jet Noise, Combustion and Car Engine Noise*, Vol. 43, edited by I. R. Schwartz, New York, 1976, pp. 137-158.

[10]Goodykoontz, J., von Glahn, U., and Dorsch, R., "Forward Velocity Effects on Under-the-Wing Externally Blown Flap Noise," AIAA Paper 75-476, 1975; also AIAA *Progress in Astronautics and Aeronautics—Aeroacoustics: STOL Noise; Airframe and Airfoil Noise*, Vol. 45, edited by I. R. Schwartz, New York, 1976, pp. 147-174.

[11]Brooks, J. R. and Woodrow, R. J., "The Effects of Forward Speed on a Number of Turbojet Exhaust Silencers," AIAA Paper 75-506, 1975; also AIAA *Progress in Astronautics and Aeronautics —Aeroacoustics: Jet Noise, Combustion and Car Engine Noise*, Vol. 43, edited by I. R. Schwartz, New York, 1976, pp. 439-457.

[12]Cocking, B. J. and Bryce, W. D., "Subsonic Jet Noise in Flight Based on Some Recent Wind Tunnel Results," AIAA Paper 75-462, 1975.

[13]Jeffery, R. W. and Holbeche, T. A., "An Experimental Investigation of Noise-Shielding Effects for a Delta-Winged Aircraft in Flight, Wind Tunnel and Anechoic Room," AIAA Paper 75-513, 1975; also AIAA *Progress in Astronautics and Aeronautics —Aeroacoustics: STOL Noise; Airframe and Airfoil Noise*, Vol. 45, edited by I. R. Schwartz, New York, 1976, pp. 419-440.

[14]Holbeche, T. A. and Williams, J., "Acoustic Considerations for Noise Experiments at Model Scale in Subsonic Wind Tunnels," AGARD Rept. No. 601 (1973), pp. 8-1 to 8-30.

[15]Williams, J., "Problems of Noise Testing in Ground-Based Facilities with Forward-Speed Simulation," Presented at AGARD Flight Dynamics Panel Symposium on Flight/Ground Testing Facilities Correlation at Modane-Valloire (France), June 1975.

[16]Armstrong, F. W. and Williams, J., "Some Research Towards Quieter Aircraft," RAS Symposium on The Impact of Economics on the Design and Operation of Quieter Aircraft, April 1975.

[17]Grosche, F.-R., "Distributions of Sound Source Intensities in Subsonic and Supersonic Jets," AGARD CP 131, 1974, pp. 4-1 to 4-10.

[18]Grosche, F.-R., Jones, J. H., and Wilhold, G. A., "Measurements of the Distribution Sound Source Intensities in Turbulent Jets," AIAA *Progress in Astronautics and Aeronautics —Aeroacoustics: Jet and Combustion Noise; Duct Acoustics*, Vol. 37, edited by H. T. Nagamatsu, New York, 1975, pp. 79-92.

[19]Riegels, F. W. and Wuest, W., "Der 3m-Windkanal der Aerodynamischen Versuchsanstalt Göttingen," *Z. Flugwiss*, Vol. 9, 1961, pp. 222-228.

[20]Fütterer, H., Mehmel, D., and Riegels, F. W., "Meβtechnik, Datenerfassung und Datenverarbeitung an den groβen Windkanälen der Aerodynamischen Versuchsanstalt Göttingen," Jb. DGLR 1970 (1971), pp. 166-185.

[21]Sommerfeld, A., "Vorlesungen über theoretische Physik, Bd. IV: Optik," Akad. Verlagsges. Gest & Portig K.-G., 3. Aufl. Leipzig, 1964.

[22]Amiet, R. K., "Correction of Open Jet Wind Tunnel Measurements for Shear Layer Refraction," AIAA Paper 75-532, 1975; also AIAA *Progress in Astronautics and Aeronautics —Aeroacoustics: Acoustic Wave Propagation; Aircraft Noise Prediction; Aeroacoustic Instrumentation*, Vol. 46, edited by I. R. Schwartz, New York, 1976, pp. 259-280.

[23]Schmidt, D. W., "Recent Experimental Investigations on the Scattering of Sound by Turbulence," AGARD Rept. 461, 1963.